

Bis(bidentate) catecholamide ligands (Scheme 2) were synthesized according to previously published procedures.<sup>[20]</sup> Libraries were obtained following a simple procedure: H<sub>4</sub>-L<sup>2</sup> (33.1 mg, 0.077 mmol), H<sub>4</sub>-L<sup>3</sup> (39.0 mg, 0.077 mmol), Et<sub>4</sub>NCl, (4.3 mg, 0.026 mmol), and [Ga(acac)<sub>3</sub>] (acac = acetylacetonate) (37.1 mg, 0.102 mmol) were suspended in methanol (20 mL). A 0.5 N NaOH solution (620 μL) in H<sub>2</sub>O was added slowly, and a clear solution was obtained. After the mixture had been stirred for 2 h, the solvent was reduced to 4 mL, and excess acetone was added to precipitate the product, which was collected by ultracentrifugation, washed with acetone and dried (quantitative yields). The same library was obtained by mixing solutions of [Ga<sub>4</sub>L<sub>6</sub><sup>2</sup> ⊃ (Et<sub>4</sub>N)]<sup>11-</sup> and [Ga<sub>4</sub>L<sub>6</sub><sup>3</sup> ⊃ (Et<sub>4</sub>N)]<sup>11-</sup> at pD 7.5 after heating for several hours at 60 °C.

Received: October 2, 2000 [Z15897]

- [1] J. Lowe, D. Stock, R. Jap, P. Zwickl, W. Baumeister, R. Huber, *Science* **1995**, 268, 533.
- [2] M. Groll, L. Ditzel, J. Löwe, D. Stock, M. Bochtler, H. D. Bartunik, R. Huber, *Nature* **1997**, 386, 463.
- [3] M. Fujita, *Chem. Soc. Rev.* **1998**, 27, 417.
- [4] a) D. L. Caulder, K. N. Raymond, *J. Chem. Soc. Dalton Trans.* **1999**, 1185; b) D. L. Caulder, K. N. Raymond, *Acc. Chem. Res.* **1999**, 32, 975.
- [5] S. Leininger, B. Olenyuk, P. J. Stang, *Chem. Rev.* **2000**, 100, 853.
- [6] C. Brückner, R. E. Powers, K. N. Raymond, *Angew. Chem.* **1998**, 110, 1937; *Angew. Chem. Int. Ed.* **1998**, 37, 1837.
- [7] T. Beissel, R. E. Powers, T. N. Parac, K. N. Raymond, *J. Am. Chem. Soc.* **1999**, 121, 4200.
- [8] D. L. Caulder, R. E. Powers, T. N. Parac, K. N. Raymond, *Angew. Chem.* **1998**, 110, 1940; *Angew. Chem. Int. Ed.* **1998**, 37, 1840.
- [9] D. W. Johnson, J. Xu, R. W. Saalfrank, K. N. Raymond, *Angew. Chem.* **1999**, 111, 3058; *Angew. Chem. Int. Ed.* **1999**, 38, 2882.
- [10] J. Xu, K. N. Raymond, *Angew. Chem.* **2000**, 39, 2745; *Angew. Chem. Int. Ed.* **2000**, 112, 2857.
- [11] A combinatorial library of hydrogen-bonded tetramers was recently characterized by ESIMS: F. Hof, C. Nuckolls, J. Rebek, Jr., *J. Am. Chem. Soc.* **2000**, 122, 4251.
- [12] Six ligands with four metals can give 16710 different arrangements for a total of 152496 diastereomers. If the possibility of heteroconfigurational metal centers is considered, 2488212 possible diastereomers can be formed: 152496 for ΔΔΔΔ/AAAA (T), 840420 for ΔΔΔΔ (S<sub>4</sub>), and 1495296 for ΔΔΔΔ/AAAA (C<sub>3</sub>). With six different ligands in equimolar amounts and one metal cation, 4236 homoconfigurational diastereomers can be formed, out of which 3590 each has a probability of 0.02572% to form, 540 form with a probability of 0.01286%, and all others (106) have an abundance of 0.006% or below. For the ΔΔΔΔ assemblies, out of 12006 possible diastereomers, 11340 (94.5%) have a probability (0.0086%) to be formed; for the ΔΔΔΔ assemblies, out of 15576 diastereomers, 15540 have an abundance of 0.00643% each.
- [13] A pool of *k* different components can form *n*-assemblies in *k<sup>n</sup>* different ways. The invariance under all symmetry transformations of the point group of the *n* assembly can be used to sort out identical structures in order to draw and calculate the statistical weight of all *n* assemblies.
- [14] M. G. Marshall, C. L. Hendrickson, G. S. Jackson, *Mass Spectrom. Rev.* **1998**, 17, 1.
- [15] S. König, C. Brückner, K. N. Raymond, J. A. Leary, *J. Am. Soc. Mass Spectrom.* **1998**, 9, 1099.
- [16] G. Hopfgartner, F. Vilbois, C. Piguet, *Rapid Commun. Mass Spectrom.* **1999**, 13, 302.
- [17] In this model with ligands A and B, we assume that the rate-limiting step is the dissociation of a ligand and that the dissociation rate *k* (*k* ≪ *k'*) is identical for both ligands. The probability of incorporating a ligand is then proportional to the molar fraction of A (denoted *a*) and B (denoted *b*) in the solution. *a* and *b* are constant and equal to the molar fraction of total A and B initially present. The equilibrium can then be expressed in terms of the linear differential equations [Eqs. (3)–(8)], which are used to trace the concentration curves (Figure 4)

$$\frac{d}{dt}[A_6] = k \left[ -b[A_6] + \frac{1}{6}a[A_5B] \right] \quad (3)$$

$$\frac{d}{dt}[A_5B] = k \left[ \frac{1}{3}a[A_4B_2] + b[A_6] - \left( \frac{5}{6}b + \frac{1}{6}a \right) [A_5B] \right] \quad (4)$$

$$\frac{d}{dt}[A_3B_3] = k \left[ \frac{2}{3}a[A_2B_4] + \frac{2}{3}b[A_4B_2] - \left( \frac{1}{2}b + \frac{1}{2}a \right) [A_3B_3] \right] \quad (5)$$

$$\frac{d}{dt}[A_4B_2] = k \left[ \frac{5}{6}a[A_3B_3] + \frac{1}{2}b[A_3B_3] - \left( \frac{1}{3}b + \frac{2}{3}a \right) [A_4B_2] \right] \quad (6)$$

$$\frac{d}{dt}[AB_5] = k \left[ a[B_6] + \frac{1}{3}b[A_2B_4] - \left( \frac{1}{6}b + \frac{1}{6}a \right) [AB_5] \right] \quad (7)$$

$$\frac{d}{dt}[B_6] = k \left[ -a[B_6] + \frac{1}{6}b[AB_5] \right] \quad (8)$$

- [18] D. L. Caulder, K. N. Raymond, *Angew. Chem.* **1997**, 109, 1508; *Angew. Chem. Int. Ed. Engl.* **1997**, 36, 1439.
- [19] We did not observe the *y* = 4, *z* = 2 combination, even though we had detected this species in the binary mixture previously.
- [20] S. P. Gaucher, J. A. Leary, *Anal. Chem.* **1998**, 70, 3009.
- [21] J. Kriesel, S. Koenig, M. Freitas, A. Marshall, J. A. Leary, T. D. Tilley, *J. Am. Chem. Soc.* **1998**, 120, 12207.
- [22] U. N. Andersen, S. Koenig, M. A. Freitas, A. G. Marshall, J. A. Leary, *J. Am. Soc. Mass Spectrom.* **1998**, 10, 352.
- [23] T. D. Burns, T. G. Spence, M. A. Mooney, L. A. Posey, *Chem. Phys. Lett.* **1996**, 258, 669.
- [24] K. Wang, G. W. Gokel, *J. Org. Chem.* **1996**, 61, 4693.
- [25] J.-M. Lehn, *Chem. Eur. J.* **1999**, 5, 2455.
- [26] T. N. Parac, D. L. Caulder, K. N. Raymond, *J. Am. Chem. Soc.* **1998**, 120, 8003.

## Shape Selectivity in Hydrocarbon Conversion\*\*

Merijn Schenk, Berend Smit,\* Thijs J. H. Vlugt, and Theo L. M. Maesen

Molecular sieves with three-dimensional framework structures find many applications in catalysis.<sup>[1, 2]</sup> A comprehensive and fundamental understanding of the product selectivity associated with these catalytic processes remains a formidable challenge of considerable practical significance.<sup>[3]</sup> Herein we focus on conversion reactions of alkanes. We demonstrate that molecular sieves favor the formation of reaction intermediates that have a shape commensurate with their pore shape.

[\*] Prof. Dr. B. Smit, M. Schenk, Dr. T. J. H. Vlugt  
Department of Chemical Engineering  
Universiteit van Amsterdam  
Nieuwe Achtergracht 166, 1018 WV Amsterdam (The Netherlands)  
Fax: (+31)20-525-5604  
E-mail: smit@its.chem.uva.nl  
Dr. T. L. M. Maesen  
Zeolyst International, PQ R&D Center  
Conshohocken, PA 19428-2240 (USA)

[\*\*] These investigations were supported in part by the Netherlands Research Council for Chemical Sciences (CW) with financial aid from the Netherlands Technology Foundation and by the Netherlands Organization for Scientific Research (NWO) through PIONIER. We would like to thank Christa Roemkens, Rob van Veen, Henk Schenk, Daan Frenkel, David Dubbeldam, and Marcello Rigutto for their comments on our manuscript.

The ultimate fate of these intermediates depends on whether diffusion, hydrocracking, or methyl shifts have the lowest Gibbs free energy barrier. We obtain microscopic information on the adsorbed molecules using configurational-bias Monte Carlo simulations. This information on a molecular level enables the explanation of peculiarities in known product distributions.<sup>[4–6]</sup>

The conversion of linear alkanes can be described as a series of consecutive reactions each increasing the degree of branching (monobranched, dibranched, etc.).<sup>[7]</sup> Methyl shifts can transfer these molecules into isomers with the same number of branches. Together with this increasing degree of branching, consecutive hydroisomerization reactions increasingly compete with hydrocracking reactions that decompose the molecule. The overall mechanism is therefore a very complex scheme with many different reaction intermediates.<sup>[8]</sup> The products of the reaction are a mixture of the various isomers and their hydrocracking products and can be seen as a fingerprint of the molecular sieve.

To arrive at a general mechanism that can explain the shape-selective conversion of alkanes we assume that the Polanyi–Brønsted principle holds. This principle implies that equilibrium thermodynamics reflect the relative probability of formation of a particular isomer, provided it is formed through the same reaction mechanism as other, competing isomers.<sup>[9, 10]</sup> Whether this isomer will appear in the product distribution depends on the relative rates of diffusion and of consecutive reactions (hydrocracking or hydroisomerization). Since isomers with the branches at the same carbon atom or at carbon atoms one methylene ( $\text{CH}_2$ ) group apart undergo hydrocracking three orders of magnitude faster than the other isomers,<sup>[8]</sup> we assume that hydrocracking occurs only through these isomers.

Differences in the Gibbs free energy of formation determine the equilibrium concentration of the various reaction intermediates. If we use the tabulated free energies of formation in the gas phase,<sup>[11]</sup> we would predict that all routes contribute comparably to the overall conversion and that all branched isomers will form. In fact, such a product distribution is observed in the FAU-type zeolite, which indicates that this large-pore zeolite does not modify the thermodynamic product distribution.<sup>[7, 8]</sup> However, by using gas-phase thermodynamics, we implicitly assume that the change in Gibbs free energy for the transfer of a molecule from the gas phase into the sieve

is similar for all reaction intermediates. For the large FAU-type pores<sup>[12]</sup> this is a reasonable assumption, but not for zeolites with smaller pores. Since the contribution of the sieve to the free energies of formation cannot always be obtained from available experimental data, we use configurational-bias Monte Carlo (CBMC) simulations<sup>[13a]</sup> to compute the contribution of the zeolites to the free energies of formation.

Figure 1 shows the contribution of several zeolites to the Gibbs free energy of formation of the various reaction intermediates involved in decane conversion. The differences between the various isomers in the gas phase are relatively small ( $5 \text{ kJ mol}^{-1}$  at most).<sup>[11]</sup> Similar differences are found in the FAU-type zeolite. Large differences in the Gibbs free energy between the various intermediates are observed in MFI-, MEL-, and TON-type zeolites. For example, the Gibbs free energy of formation of the tri-branched alkanes with proximate methyl groups is very large. The formation of these isomers will therefore be suppressed.<sup>[9, 10]</sup> In this way the Gibbs free energy modifications afford an unambiguous assessment of the possibility for shape selectivity of the transition state. Experimentally, such an assessment has often proved to be difficult.<sup>[3]</sup>

To investigate the mobility of a reaction intermediate we have computed the Gibbs free energy of this molecule as a function of its position in the sieve.<sup>[14]</sup> If this Gibbs free energy profile shows barriers that are much larger than the thermal energy ( $\gg 1k_{\text{B}}T$ ), diffusion will be slowed down by the zeolite. In MEL- and MFI-type zeolites, mono-methyl alkanes have a

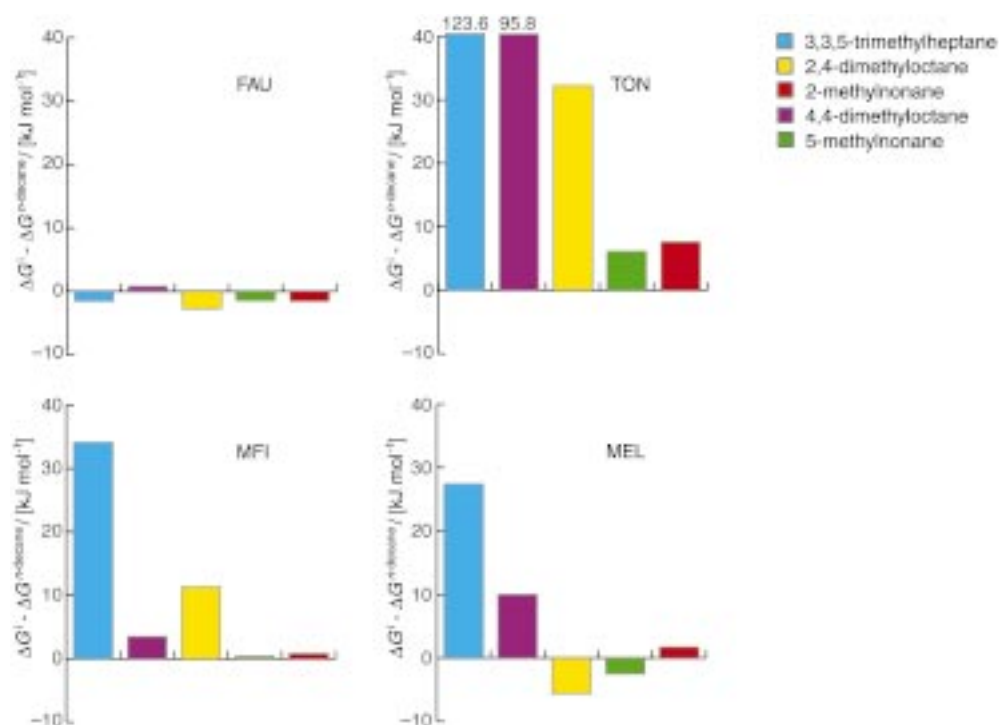


Figure 1. The Gibbs free energy of formation of hydrocarbons relative to decane in FAU-, TON-, MFI-, and MEL-type sieves as obtained from CBMC simulations.<sup>[13b]</sup> The interaction parameters used in this study can reproduce the experimental adsorption isotherms of linear and branched alkanes in various zeolites accurately.<sup>[13a]</sup> The changes in the Gibbs free energy were calculated using one molecule at infinite dilution at  $T = 415 \text{ K}$ . At this temperature the Gibbs free energy of formation of all  $\text{C}_{10}$  isomers in the gas phase is  $(149 \pm 2) \text{ kJ mol}^{-1}$ . Only the isomers with the greatest influence on the product distribution are shown. Details on the technique and the model can be found in Vlugt et al.<sup>[13a]</sup>

barrier of  $12\text{--}14k_{\text{B}}T$ , while in TON-type zeolites it is only  $6k_{\text{B}}T$ . These values indicate that diffusion rates of mono-methyl alkanes are lower in MEL- or MFI-type zeolites than in TON-type zeolites. Quantitatively similar results were obtained from molecular dynamics simulations.<sup>[15, 16]</sup> The Gibbs free energy profiles of some di-branched isomers in MEL and MFI are compared in Figure 2. These results indicate that the dimethylalkanes have a barrier of  $15\text{--}60k_{\text{B}}T$ , which results in diffusion coefficients ranging from  $10^{-16}$  to  $10^{-32}\text{ m}^2\text{ s}^{-1}$ . These diffusion coefficients are too low to be calculated by molecular dynamics simulations.<sup>[15, 16]</sup>

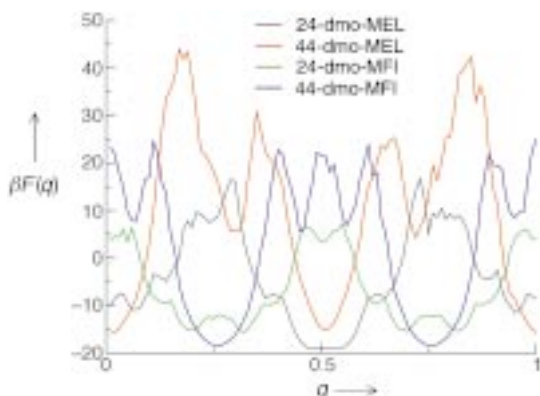


Figure 2. Gibbs free energy (in units of  $k_{\text{B}}T$ ) as a function of the position of the  $n,m$ -dimethyloctane (dmo) isomers in MEL- and MFI-type zeolites. We have limited the calculation to the straight channel for MFI-type zeolites; similar results are obtained for a zigzag channel. Instead of calculating the average Gibbs free energy of a molecule in a zeolite (as is done in Figure 1), we compute the Gibbs free energy as a function of the position of the molecule along a channel. The parameter  $q$  is the fractional coordinate with respect to the unit cell of the 3-position of the chain in the case of 2,4-dmo and the 4-position in case of 4,4-dmo. The middle of the intersections in a MEL-type zeolite have reduced coordinates of  $q = 0.25$  and  $q = 0.75$  and in an MFI-type zeolite of  $q = 0$ ,  $q = 0.5$ , and  $q = 1$ . The reported diffusion coefficients have been calculated using these Gibbs free energy profiles assuming that transition-state theory holds.

An explanation for the high hydrocracking selectivity of MEL- and MFI-type zeolites relative to TON- or FAU-type zeolites is that the former selectively reduce the Gibbs free energy of formation of those dimethylalkanes that hydrocrack most easily. Dimethylalkanes with methyl groups attached to the same carbon atom or separated by one methylene ( $\text{CH}_2$ ) group hydrocrack more quickly than other dimethylalkanes because they form both secondary and tertiary carbocation transition states instead of only secondary carbocation transition states.<sup>[5, 7]</sup> The formation of these isomers is enhanced, because their shape is commensurate with that of the pore intersection: 4,4-dimethyloctane fits snugly when it has its octane backbone in the straight MFI-type channel and the two methyl groups in the zigzag channel; 2,4-dimethyloctane on the other hand has a perfect fit in the large MEL-type intersection because the distance between the two branches matches the distance between the two intersecting channels. Those intermediates that are commensurate with the zeolite structure are preferentially formed but cannot diffuse out of the zeolite without being hydrocracked. Since hydrocracking of 2,4-dimethyloctane yields isobutane, while hydrocracking

of 4,4-dimethyloctane yields *n*-butane,<sup>[7]</sup> we now understand why the conversion of *n*-decane using MEL-type zeolites yields about twice as much isobutane as that using MFI-type zeolites.<sup>[4, 5]</sup> In this case the thermodynamic and diffusion properties can only be calculated: the dimethyloctanes studied diffuse too slowly to be amenable to traditional adsorption experiments.

We can apply this procedure to determine general trends in a product distribution for other hydrocarbon conversion processes. The aim of dewaxing is to transfer long-chain hydrocarbons (waxes) into branched isomers. Hydrocracking is an undesirable side reaction that we would like to suppress as much as possible. Figure 1 shows that the dimethylalkanes that most easily hydrocrack (alkanes with proximate methyl groups) have a relatively high Gibbs free energy of formation in TON-type zeolites. Figure 3 shows that TON-type zeolites

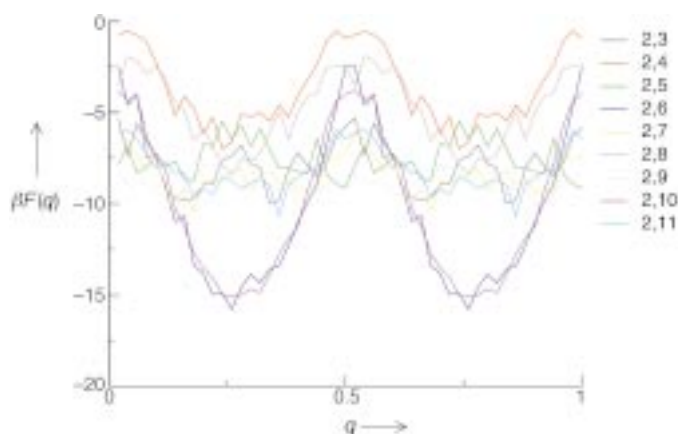


Figure 3. Gibbs free energy as a function of the position of the  $2,m$ -dmpd isomers in TON-type zeolites (see also the caption to Figure 2).

instead favor the formation of di-branched alkanes with the methyl group separated by two or more methylene groups. 2,6- and 2,10-dimethylpentadecane (dmpd) have the lowest Gibbs free energy of formation. The shape of these two isomers is commensurate with the periodicity of the cavities in the TON-type zeolite channel (Figure 4). There is no such perfect match between the spacing of the methyl groups and that of the undulations in the TON-type channels for the other isomers. Figure 3 shows that commensurate 2,6- and 2,10-dmpd have a barrier of  $15k_{\text{B}}T$ , which gives a diffusion coefficient of  $2 \times 10^{-13}\text{ m}^2\text{ s}^{-1}$ , and shows that the diffusion of the incommensurate 2,7- or 2,9-dmpd is virtually unhampered. From this Figure we can deduce the Gibbs free energy of formation of the various  $2,m$  isomers. The incommensurate isomers have similar Gibbs free energies while the commensurate 2,6-dmpd has a Gibbs free energy of formation  $5k_{\text{B}}T$  lower. The barrier for all methyl shifts is only  $1.5k_{\text{B}}T$  in the gas phase or in a wide-pore zeolite.<sup>[8]</sup> The Polanyi–Brønsted principle suggests that TON-type zeolites raise this barrier (by some  $5k_{\text{B}}T$ ) for the methyl shift of a commensurate isomer (2,6-dmpd) into an incommensurate one (2,5- or 2,7-dmpd), but leave the methyl shifts among incommensurate isomers unaffected. The reason for the relatively high barriers to diffusion of the commensurate intermediates is that the

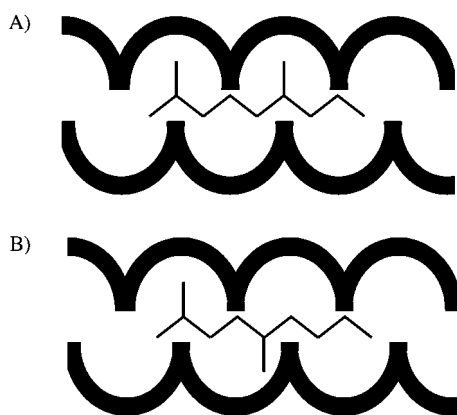


Figure 4. Sketch of a commensurate (A) and an incommensurate (B) molecule in a TON-type zeolite. If there are three carbon atoms separating the two methyl groups the molecule is commensurate with the zeolite structure. If we displace, for example, a 2,6-dimethylpentadecane (dmpd) isomer both methyl groups have to leave their optimal position. If we displace an incommensurate molecule, for example, the 2,5-dmpd isomer, part of the molecule always remains in an unfavorable configuration. As a consequence, the Gibbs free energy barriers of the incommensurate molecules are much smaller and hence these molecules diffuse faster.

diffusion of a commensurate isomer requires that both methyl groups leave their thermodynamically favorable sites, while the diffusion of an incommensurate molecule always involves one methyl group at an unfavorable position. Therefore a displacement of a commensurate molecule changes the Gibbs free energy more than that of an incommensurate molecule. A similar effect has been observed for clusters of molecules.<sup>[17]</sup>

These simulation results lead to the following hydrocarbon conversion mechanism: The commensurate 2,6- and 2,10-dmpd will form preferentially but their barrier for diffusion is higher than their barrier for a methyl shift. Once a methyl shift has taken place, an incommensurate structure has formed which can leave the zeolite. However, 2,5-dmpd can easily undergo a methyl shift into 2,4-dmpd, which will hydrocrack before it leaves the zeolite. This suggests that in the product slate we may find some 2,5-, very little 2,6-, but a significant amount of 2,7-, 2,8-, and 2,9-dmpd isomers. Aspects of such a product distribution have been observed experimentally. Interestingly, these effects were explained in terms of catalysis at the exterior zeolite surface<sup>[6]</sup> (“pore mouth” and “key lock” catalysis). Our interpretation implies catalysis inside the zeolitic pores. A similar conclusion has been obtained from molecular dynamics simulations.<sup>[15, 16, 18]</sup> We have also calculated the Gibbs free energy profiles of the 3,*m*-dmpd isomers. For these isomers we find that 3,7-dmpd is the commensurate molecule. The Gibbs free energy of these 3,*m* isomers is  $1-2k_B T$  higher than that of the 2,*m* isomers. We therefore expect that the product distribution also contains 3,8-, 3,9-, and 3,10-dmpd isomers in slightly smaller quantities.

It is instructive to compare our approach and the traditional concepts in shape-selective catalysis (reactant, transition state, and product shape selectivity<sup>[3, 19, 20]</sup>). When a reactant is excluded from a zeolite (reactant selectivity), this is reflected by a very high Gibbs free energy of adsorption in our simulations.<sup>[18]</sup> When the formation of a product or

intermediate is impeded or favored (transition state<sup>[19]</sup> or inverse<sup>[21]</sup> shape selectivity) the Gibbs free energy of such a molecule increases or decreases, respectively. When the diffusion rate of one product is slow relative to that of another (product shape selectivity<sup>[20]</sup>) this shows up in the Gibbs free energy profile. Thus, CBMC calculations give a complete picture of shape selectivity, something that is very difficult experimentally.

An important concept in this work is whether a molecule is commensurate with the zeolite structure. The diffusion and thermodynamic characteristics of molecules whose shape is commensurate with that of the zeolite pore is very different from that of the incommensurate ones. These subtle differences have remarkably large influence on the product distribution.

Received: October 26, 2000 [Z16000]

- [1] P. M. M. Blauwhoff, J. W. Gosselink, E. P. Kieffer, S. T. Sie, W. H. J. Stork in *Catalysis and Zeolites* (Eds.: J. Weitkamp, L. Puppe), Springer, Berlin, **1999**, pp. 437–538.
- [2] K. Tanabe, W. F. Hölderich, *Appl. Catal.* **1999**, *181*, 399–434.
- [3] J. Weitkamp, S. Ernst, L. Puppe in *Catalysis and Zeolites* (Eds.: J. Weitkamp, L. Puppe), Springer, Berlin, **1999**, pp. 327–370.
- [4] P. A. Jacobs, J. A. Martens, J. Weitkamp, H. K. Beyer, *Faraday Discuss. Chem. Soc.* **1982**, *72*, 353–369.
- [5] J. Weitkamp, P. A. Jacobs, J. A. Martens, *Appl. Catal.* **1983**, *8*, 123–141.
- [6] J. A. Martens, W. Souverijns, W. Verrelst, R. Parton, G. F. Froment, P. A. Jacobs, *Angew. Chem.* **1995**, *101*, 2726–2728; *Angew. Chem. Int. Ed. Engl.* **1995**, *34*, 2528–2530.
- [7] J. A. Martens, P. A. Jacobs in *Theoretical Aspects of Heterogeneous Catalysis* (Ed.: J. B. Moffat), Van Nostrand Reinhold, New York, **1990**, pp. 52–109.
- [8] G. Martens, G. F. Froment in *Reaction Kinetics and the Development of Catalytic Processes* (Eds.: G. F. Froment, K. C. Waugh), Elsevier, Amsterdam, **1999**, pp. 333–340.
- [9] R. A. Van Santen, J. W. Niemantsverdriet, *Chemical Kinetics and Catalysis*, Plenum, New York, **1995**, pp. 197–201.
- [10] B. C. Gates, *Catalytic Chemistry*, Wiley, New York, **1992**, pp. 26–31.
- [11] D. R. Stull, E. F. Westrum, G. C. Sinke, *The Chemical Thermodynamics of Organic Compounds*, 2nd ed., Krieger, Malabar, FL, **1987**.
- [12] W. M. Meier, D. H. Olson, C. Baerlocher, *Atlas of Zeolite Structure Types* 4th ed., Elsevier, London, **1996**; www.iza-structure.org/databases/ by C. Baerlocher, L. B. McCusker.
- [13] a) T. J. H. Vlucht, R. Krishna, B. Smit, *J. Phys. Chem. B* **1999**, *103*, 1102–1118; b) in a CBMC simulation molecules are grown atom-by-atom; the so-called Rosenbluth factor is calculated during the growing process. This factor  $W_{\text{sieve}}$  is directly related to the Gibbs free energy of the molecule in the molecular sieve. By using the same technique we can calculate the Rosenbluth factor of a molecule in the ideal gas phase,  $W_{\text{gas}}$ . The Gibbs free energy difference between a molecule in the sieve and one in the ideal gas phase follows the ratio of these Rosenbluth factors:  $\Delta G^{\text{sieve}} = G^{\text{sieve}} - G^{\text{gas}} = -RT \ln(W_{\text{sieve}}/W_{\text{gas}})$ .
- [14] B. Smit, L. D. J. C. Loyens, G. L. M. M. Verbist, *Faraday Discuss.* **1997**, *106*, 93–104.
- [15] E. B. Webb III, G. S. Grest, *Catal. Lett.* **1998**, *56*, 95–104.
- [16] E. B. Webb III, G. S. Grest, M. Modello, *J. Phys. Chem. B* **1999**, *103*, 4949–4959.
- [17] D. S. Sholl, K. A. Fichthorn, *Phys. Rev. Lett.* **1997**, *79*, 3569–3572.
- [18] T. L. M. Maesen, M. Schenk, T. J. H. Vlucht, J. P. De Jonge, B. Smit, *J. Catal.* **1999**, *188*, 403–412.
- [19] S. M. Csicsery, *Zeolites* **1984**, *4*, 202–213.
- [20] P. Weisz, *Pure Appl. Chem.* **1980**, *52*, 2091–2103.
- [21] D. S. Santilli, T. V. Harris, S. I. Zones, *Microporous Materials* **1993**, *1*, 329–341.